Università di Pisa

Design Criteria for the RF Section of UHF and Microwave Passive RFID Transponders

Giuseppe De Vita
Dipartimento di Ingegneria dell'Informazione: Elettronica, Informatica, Telecomunicazioni, Università di Pisa
Giuseppe Iannaccone
Dipartimento di Ingegneria dell'Informazione: Elettronica, Informatica, Telecomunicazioni, Università di Pisa

G. De Vita, G. Iannaccone, *Design Criteria for the RF Section of UHF and Microwave Passive RFID Transponders,* IEEE Trans. Microwave Theory and Techniques, **53**, pp.2978-2990 (2005).

Design Criteria for the RF Section of UHF and Microwave Passive RFID Transponders

Giuseppe De Vita and Giuseppe Iannaccone, *Member, IEEE*

***Abstract*—A set of design criteria for the radio-frequency (RF) section of long-range passive RF identification (RFID) transponders operating in the 2.45-GHz or 868-MHz industrial, scientific, and medical (ISM) frequency ranges is derived in this paper, focusing in particular on the voltage multiplier, the power-matching network, and the backscatter modulation. The paper discusses the design tradeoffs between the error probability at the reader receiver and the converted RF–dc power at the transponder, determining the regions of the design space that allow optimization of the operating range and the data rate of the RFID system.**

***Index Terms*—Backscatter modulation, passive transponders, radio-frequency identification (RFID), RF rectifier.**

I. Introduction

LONG-RANGE passive transponders ("tags") for radio frequency identification (RFID) systems do not have an on-board battery and therefore must draw the power required for their operation from the electromagnetic field transmitted by the reader [1]. The RF energy radiated by the reader is used both to supply the digital section of the transponder and to allow data transmission from the tag to the reader through modulation of the backscattered radiation. If the transponder lies within the interrogation range of the reader, an alternating RF voltage is induced on the transponder antenna and is rectified in order to provide a dc supply voltage for transponder operation. In order to further increase the supply voltage, an N-stage voltage multiplier is typically used, providing a dc output voltage, at constant input power, roughly N times larger than that achievable with a single stage. In addition, most of the passive and semipassive RFID systems that operate in the ultra-high-frequency (UHF) or microwave range exploit modulation of the backscattered radiation to transmit data from transponder to reader: while the reader transmits a unmodulated carrier, the data signal modulates the load of the transponder antenna in order to modulate the backscattered electromagnetic field, typically with amplitude-shift keying (ASK) or phase-shift keying (PSK) [1].

It is apparent that the larger the modulation of the impedance seen by the antenna, the larger the modulation depth and the signal-to-noise ratio at the reader, but also the larger the mismatch, and therefore the smaller the dc power converted by the voltage multiplier.

In order to maximize the operating range, it is important to achieve a nontrivial tradeoff between the desired error probability at the reader and the dc power available for supplying the transponder, which is also strongly dependent on the power efficiency of RF–dc conversion.

The maximization of the conversion efficiency requires the optimization of the voltage multiplier and of the power-matching network, taking into account the nonlinear behavior of the voltage multiplier.

The architecture of a passive microwave RFID transponder is shown in Fig. 1. The coupling element is an antenna, which typically is a dipole or a patch antenna. A voltage multiplier converts the input alternating voltage into a dc voltage, which is used by a series voltage regulator to provide the regulated voltage required for the correct operation of the transponder. The voltage multiplier is matched with the antenna in order to ensure the maximum power transfer from the transponder's antenna to the input of the voltage multiplier. A backscatter modulator is used to modulate the impedance seen by the transponder's antenna, when transmitting. The RF section is then connected to the digital section, which typically is a very simple microprocessor or a finite-state machine able to manage the communication protocol.

This paper presents a set of design criteria for the RF section of passive transponders in the UHF and microwave frequency range, referring to the architecture shown in Fig. 1, with the main objective of maximizing the operating range. The focus, therefore, is on the optimization of the voltage multiplier and on its power matching to the antenna, and a set of criteria is derived that allows the choice and optimization of backscatter modulation in order to either maximize the operating range, once the data rate is fixed, or maximize the data rate, once the operating range is fixed.

In the remainder of the paper, all numerical examples will refer to the 0.35-mm complementary metal–oxide–semiconductor (CMOS) technology from AMS, but of course the considerations can be applied to any technology.

This investigation will show that, for a passive RFID system compliant to European regulations in the 2.45-GHz or 868-MHz ISM frequency bands, the achievable operating range, considering a power consumption of the digital section of the transponder of 1 μW, is larger than 4 and 11 m, respectively. At the same time, it will be shown that, for a passive 2.45-GHz RFID system, given an operating range of 4 m, the achievable data rate is about 30 kb/s, and for a passive 868-MHz RFID system, given an operating range of 11 m, the achievable data rate is about 180 kb/s. Considering the more permissive U.S. regulations, the maximum achievable operating distances are 11 m in the 2.45-GHz frequency band and 29 m at 916 MHz, considering a data rate of some tens of kilobits per second.

The extremely low power consumption considered for the digital logic is achievable by using subthreshold logic schemes,

Manuscript received December 15, 2004; revised April 29, 2005. This work was supported by the Fondazione Cassa di Risparmio di Pisa.

The authors are with the Dipartimento di Ingegneria dell'Informazione, 56122 Pisa, Italy (e-mail: giuseppe.devita@iet.unipi.it; giuseppe.iannaccone@iet.unipi.it).

Digital Object Identifier 10.1109/TMTT.2005.854229

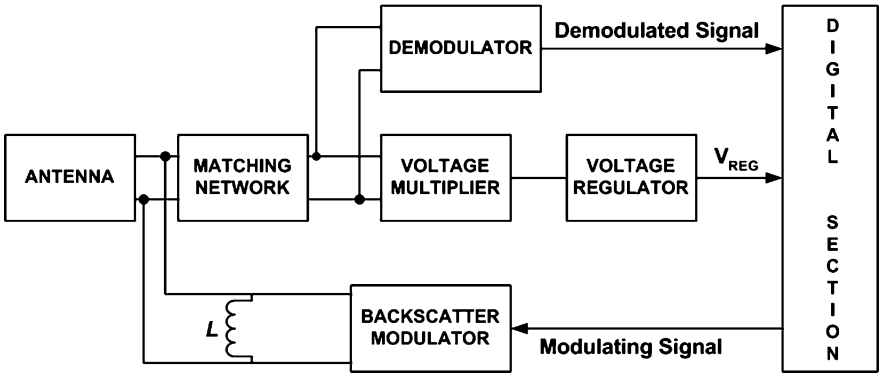

Fig. 1. Passive Transponder Architecture.

given that a simple finite-state machine operating at a frequency smaller than 1 MHz is typically adequate to implement RFID protocols. However, this aspect is beyond the scope of the present paper and will not be discussed here.

II. Voltage Multiplier and Power Matching Network

In this section, we will describe the design criteria for both the voltage multiplier and the power-matching network in order to maximize the power efficiency of the transponder, defined as the ratio between the radio-frequency (RF) power available at the transponder's antenna and the dc power at the output of the voltage multiplier available for supplying the transponder. As we will explain in the next section, the power efficiency of the transponder strongly affects the operating range of the tag-reader system.

A. N-Stage Voltage Multiplier

An N-stage voltage multiplier consists of a cascade of N peak-to-peak detectors, as shown in Fig. 2 [2]. Let us suppose to apply, at the input of the voltage multiplier, a sinusoidal voltage $V_{\rm IN}$, with a frequency f_0 and an amplitude V_0. In order to ensure a small ripple in the output voltage V_U, the capacitors indicated with C in Fig. 2 have to be dimensioned so that their time constant is much larger than the period of the input signal, that is, $I_U/(2\pi C V_U) \ll f_0$, where I_U is the dc output current. In this way, the voltage across C capacitors and the output voltage can be considered a dc voltage. As a consequence, in the high-frequency analysis, it is possible to consider C capacitors as short-circuits and therefore all diodes appear to lie directly in parallel or antiparallel to the input. In this situation, the input RF voltage entirely drops across the diodes. In the dc analysis, C capacitors can be considered as open circuits so that we have $2N$ identical diodes in series with the output. The voltage V_d that drops across each diode is, therefore, given by

$$V_d = \pm V_0 \cos(\omega_0 t) - \frac{V_U}{2N} \tag{1}$$

where the sign "+" is applied to diodes with an even subscript (see Fig. 2) and the sign "−" is applied to diodes with an odd subscript. We can represent the equivalent circuit of the diode as an ideal diode in parallel with a capacitance C_D, as shown in Fig. 3(a), neglecting diode series resistances. Indeed, since

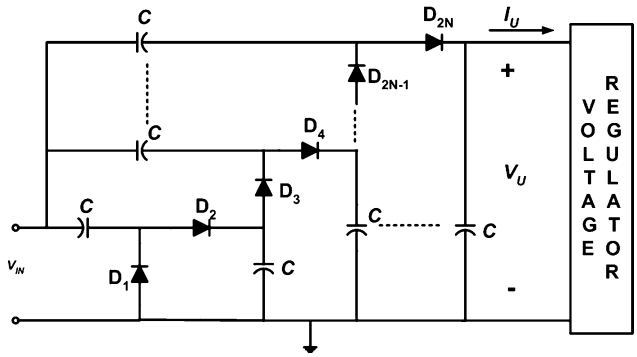

Fig. 2. N-stage voltage multiplier and cascaded series voltage regulator.

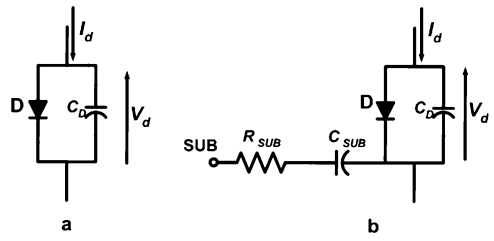

Fig. 3. Simplified equivalent circuit of the considered diodes: (a) substrate losses neglected and (b) equivalent circuit including substrate losses.

the dc power required by radio-frequency identification (RFID) passive transponders is quite low (in the order of a few microwatts), the dc output current of the voltage multiplier is very small, leading to a negligible effect of the series resistance of the diodes. Such hypothesis was verified by circuit simulations. Thus, the current I_d in each diode is

$$I_d = I_S \left[\exp\left(\pm \frac{V_0}{V_T} \cos(\omega_0 t) \right) \exp\left(-\frac{V_U}{2NV_T} \right) - 1 \right] + C_D \frac{dV_d}{dt} \tag{2}$$

where I_S is the diode saturation current and V_T is the thermal voltage. We can express the exponential of a cosinusoidal function using the modified Bessel functions series expansion [3],

$$\exp(\pm x \cos(\omega t)) = B_0(\pm x) + 2 \sum_{n=1}^{\infty} B_n(\pm x) \cos(n\omega t). \tag{3}$$

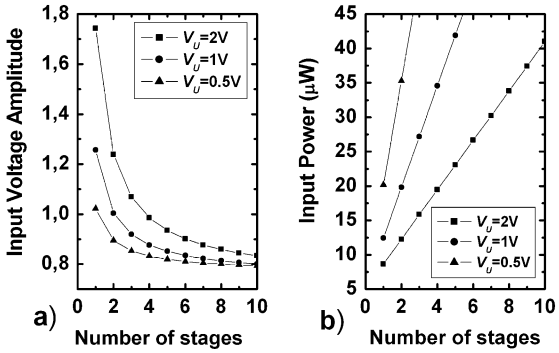

Fig. 4. (a) Required amplitude of the input voltage versus the number of stages for an output power of 5 μW. (b) Required input power versus the number of stages for an output power of 5 μW, for an I_S of 10^{-17} A.

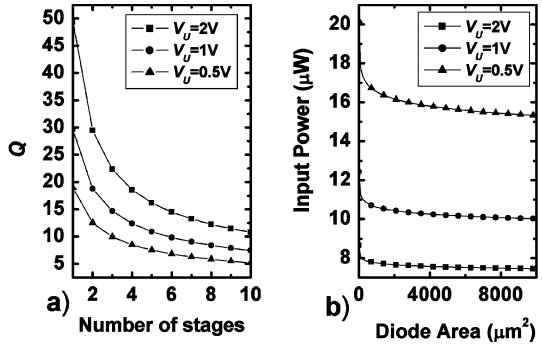

Fig. 5. (a) Required Q factor of the matching network versus the number of stages for an output power of 5 μW. (b) Average input power versus diodes area for a single-stage voltage multiplier with an output power of 5 μW.

Since modified Bessel functions of odd (even) order are odd (even) [3], the dc current in each diode, which also is the dc current I_U in the output load, is given by

$$I_U = I_S \left[B_0 \left(\frac{V_0}{V_T} \right) \exp \left(-\frac{V_U}{2NV_T} \right) - 1 \right]. \tag{4}$$

As a consequence, the input–output characteristics of the N-stage voltage multiplier is intrinsically expressed by

$$\left(1 + \frac{I_U}{I_S} \right) \exp \left(\frac{V_U}{2NV_T} \right) = B_0 \left(\frac{V_0}{V_T} \right). \tag{5}$$

The above equation can be easily solved by numerical iteration, yielding the monotonously decreasing behavior of V_0 as a function of N for fixed dc output voltage and power consumption plotted in Fig. 4(a), for an I_S of 10^{-17} A, which is the I_S for a minimum diode area in the technology we are considering. However, for large N, the curves almost saturate, since voltage multiplication is limited by the voltage drops on the diodes.

1) Power Consumption: The average input power $P_{\rm IN}$ required to obtain a given output voltage and power can be calculated by summing up the average power P_D dissipated in each diode and the power P_L required by the load. Neglecting substrate losses, the average power dissipated in each diode is given by

$$P_D = \frac{1}{T} \int_0^T V_d(t) I_d(t) dt \tag{6}$$

where T is the period of the input voltage. By solving the integral with the expressions of $V_d(t)$ and $I_d(t)$, already given in (1) and (2), and taking into account the properties of the modified Bessel functions, it is possible to obtain

$$P_D = I_S V_0 B_1 \left(\frac{V_0}{V_T} \right) \exp \left(-\frac{V_U}{2NV_T} \right) - \frac{P_L}{2N}. \tag{7}$$

As a consequence, the average input power is given by

$$\begin{aligned} P_{\rm IN} &= 2NP_D + P_L \\ &= 2NI_S V_0 B_1 \left(\frac{V_0}{V_T} \right) \exp \left(-\frac{V_U}{2NV_T} \right). \end{aligned} \tag{8}$$

Considering that V_0 is a function of N from (5), in order to obtain the plot of $P_{\rm IN}$ as a function of N, shown in Fig. 4(b), for a fixed output power, it is necessary to solve the equation by a numerical iteration. From the plot shown in Fig. 4(b), it is possible to note that the maximum power efficiency is obtained by using the minimum number of stages. In order to provide a criterion for the choice of the appropriate number of stages, we need to find a relation between the number of stages of the voltage multiplier and the Q factor of the power-matching network placed between the antenna and the voltage multiplier. We can define an equivalent input resistance of the voltage multiplier, considering the power consumption, as follows:

$$R_{\rm eq} = \frac{V_0^2}{2P_{\rm IN}}. \tag{9}$$

Now, assuming to use an *LC*-matching network, the Q factor of the *LC*-matching network is bound to the resistance transformation ratio [4], and its is given by

$$Q = \sqrt{\frac{R_{\rm eq}}{R_A} - 1} \tag{10}$$

where R_A is the antenna resistance, neglecting antenna losses. Assuming that the antenna is a dipole (antenna resistance 72 Ω [1]), from (5), (9), and (10) we plot Q as function of N in Fig. 5(a). It is clear that similar conclusions can be obtained using other types of antennas.

Although the highest efficiency is reached with only one stage, the choice of the number of stages has to be done, taking into account the values of Q that can be physically achievable, which, typically, are not larger than a few tens. A possibility to reduce the required Q is represented by the choice of antennas with higher radiation resistance, such as a two-wire or a three-wire folded dipole. Once the number of stages is chosen following the above criteria, it is necessary to dimension the diodes in order to optimize the power efficiency of the voltage multiplier. Considering that I_S is proportional to the diode area, by solving the equation $P_{\rm IN}(I_S)$ for a fixed value of N and for a certain value of the output voltage and power, one obtains the curve plotted in Fig. 5(b). It is possible to note that the higher the diode area and then the saturation current of the diodes are, the better the power efficiency of the voltage multiplier is. However, it is not possible to increase excessively the diode area; otherwise, the diode capacitance would become

comparable with the C capacitances of the voltage multiplier. This situation would lead to a reduction of the efficiency because only a fraction of the input voltage would drop across the diodes. The previous consideration suggests that the best choice would be represented by Schottky diodes, which have a higher saturation current compared with normal diodes, for a fixed area. Furthermore, since diodes in the voltage multiplier must have a switching time smaller than the period of the input signal, Schottky diodes have to be preferred because they are typically much faster than p-n diodes. However, we will focus our attention on p-n-junction diodes that have the advantage of being available in a less expensive CMOS process.

2) Power Consumption in the Presence of Substrate Losses: In order to take into consideration the substrate losses in the diodes, we can use the equivalent circuit shown in Fig. 3(b), where $R_{\rm SUB}$ and $C_{\rm SUB}$ are the substrate parasitic resistance and capacitance, respectively [2]. By substituting the equivalent circuit of the diodes into the voltage multiplier, shown in Fig. 2, we can note that the power dissipation due to substrate losses in the diodes with odd subscript is zero because the voltage that drops across the series of $R_{\rm SUB}$ and $C_{\rm SUB}$ is approximately a dc voltage. Instead, the power dissipation due to substrate losses in the diodes with an even subscript is given by

$$P_{D\rm SUB} \cong \frac{1}{2} V_0^2 R_{\rm SUB} (2\pi f_0 C_{\rm SUB})^2 \tag{11}$$

under the assumption that $2\pi f_0 R_{\rm SUB} C_{\rm SUB} \ll 1$ [2]. Thus, the average input power is obtained by summing up expression (8) previously found and the power dissipated in the diodes due to the substrate losses, as follows:

$$P_{\rm IN} = 2NI_S V_{\rm in} B_1 \left(\frac{V_0}{V_T}\right) \exp\left(-\frac{V_U}{2NV_T}\right) + NP_{D\rm SUB}. \tag{12}$$

We plotted $P_{\rm IN}(N)$ for different values of $R_{\rm SUB}(2\pi f_0 C_{\rm SUB})^2$ in Fig. 6. It is possible to note that, for increasing $R_{\rm SUB}(2\pi f_0 C_{\rm SUB})^2$, the number of stages corresponding to the minimum input power is shifted to higher values. Once $R_{\rm SUB}$ and $C_{\rm SUB}$ are known, it is possible to find the optimum number of stages in order to maximize the power efficiency of the voltage multiplier.

B. Input Equivalent Impedance

The input equivalent impedance of the voltage multiplier is constituted by the parallel of a resistance and a capacitance. From our previous considerations, the input capacitance of the voltage multiplier is the sum of the capacitances of all diodes. Since, in a voltage multiplier, diodes conduct for a very small fraction of the period of the input signal, when calculating the mean value of the diode capacitance, we can neglect the diffusion capacitance. Using the SPICE model of a p–n junction

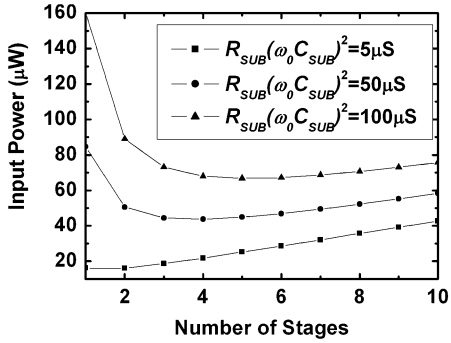

Fig. 6. Input power versus number of stages for an output voltage of 0.5 V, an output power of 5 μW, and three values of $R_{\rm SUB}(\omega C_{\rm SUB})^2$.

[5], the depletion layer capacitance C_D of a diode is given by (13) at the bottom of this page, where C_{j0} is the depletion capacitance at zero bias, m is the grading coefficient, V_γ is the built-in voltage, FC is the forward bias depletion capacitance coefficient, and A is the area of the diode [5]. Since the diode capacitance is a function of the voltage applied to the diode, we can consider the average value of the diode capacitance within the diode voltage swing, as follows:

$$\bar{C}_D = \frac{1}{2V_0} \int_{-V_0-\frac{V_U}{2N}}^{V_0-\frac{V_U}{2N}} C_D(V_d) dV_d. \tag{14}$$

Considering the average value of the capacitance of each diode, the equivalent input capacitance $C_{\rm eq}$ of the voltage multiplier, due to the diode capacitance, is given by

$$C_{\rm eq} = 2N\bar{C}_D. \tag{15}$$

The equivalent input resistance $R_{\rm eq}$ of the voltage multiplier is the resistance calculated from the power consumption with (9).

C. Power-Matching Network

Since the power at the transponder antenna varies with the distance between the reader and the transponder, power matching will be pursued in the condition of minimum power available at the antenna that still ensures correct operation of the transponder. Indeed, in the next section we will show that the transponder continues to work correctly when the power at the antenna increases even if power matching is lost. The power matching *LC* network is shown in Fig. 7, where $L = QR_A/\omega_0, C = Q/(\omega_0 R_{\rm eq})$ [4], and Q is the quality factor of the *LC* network, obtained from (10). The backscatter modulator is removed, for the moment, so that we can optimize power matching. The inductance L', shown in Fig. 7, is used in order to compensate the equivalent input capacitance $C_{\rm eq}$ of the voltage multiplier (C and L' can be substituted by a single reactance, whose sign depends on their relative value). It is clear that since $C_{\rm eq}$ is only a time-averaged capacitance, the power matching is good, provided that the variations of the

$$C_D = \begin{cases} \frac{C_{j0}A}{\left(1-\frac{V_d}{V_\gamma}\right)^m}, & V_d < (FC)V_\gamma \\ C_{j0}A(1-FC)^{-1-m}\left[1-FC(1+m)+m\frac{V_d}{V_\gamma}\right], & V_d > (FC)V_\gamma \end{cases} \tag{13}$$

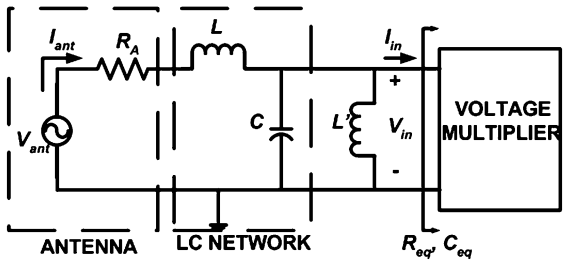

Fig. 7. Power-matching network.

input impedance of the voltage multiplier are small with respect to the average values. To verify the previous statement, we can calculate the impedance seen by the transponder's antenna in the worst matching condition, i.e., when the value of the input capacitance of the voltage multiplier is the farthest from its mean value. Referring to Fig. 7, the expressions of the real and imaginary part of the impedance Z seen by the equivalent voltage generator at the antenna $V_{\rm ant}$ can be computed as

$$\mathrm{Re}\{Z\} = \frac{R_{\rm eq}}{Q^2+1}\left[1+\frac{Q^2+1}{1+(Q\pm Q')^2}\right] \tag{16}$$

$$\mathrm{Im}\{Z\} = R_{\rm eq}\left[\frac{Q(1+(Q\pm Q')^2)-(Q\pm Q')(Q^2+1)}{(1+Q^2)(1+(Q\pm Q')^2)}\right] \tag{17}$$

where $Q' = 2\pi f_0 R_{\rm eq}\Delta C$ and ΔC is the maximum variation of the input capacitance of the voltage multiplier with respect to its mean value. In order to ensure the correct operation of the power-matching network, the real part Z has to be twice the antenna's resistance, and its imaginary part has to be zero. Such conditions are fulfilled if $Q' \ll Q$. From (16) and (17), the following condition can be derived:

$$\Delta C \ll \frac{Q}{2\pi f_0 R_{\rm eq}}. \tag{18}$$

To estimate ΔC, we can assume that the mean value of the diode capacitance is its value at the average voltage drop, i.e., $-V_U/2N$. The maximum value of the diode capacitance is obtained when $V_d = V_0 - V_U/2N$. Using an N-stage voltage multiplier, we can assume that the output voltage is $2N$ times the amplitude of the input voltage minus $2N$ times the V_γ of the diodes. As consequence, we can write the amplitude of the input voltage as $V_0 = V_U/2N + V_\gamma$.

In this condition, we can express ΔC as the difference between the maximum and the mean value of the input capacitance, i.e.,

$$\begin{aligned}\Delta C &= C_D(V_\gamma) - C_D(-V_U/2N)\\ &= 2NC_{j0}A\left[\frac{1-FC(1+m)+m}{(1-FC)^{1+m}} - \left(1+\frac{V_U}{2NV_\gamma}\right)^{-m}\right].\end{aligned} \tag{19}$$

On the one hand, once the output power and voltage are given, by substituting (19) into (18), we obtain the maximum value of the diode area that enables us to achieve power matching. On the other hand, once the output voltage and the minimum diode area are fixed, as allowed by the CMOS technology used, from (18) and (19) we can derive the maximum equivalent input resistance $R_{\rm eq\,max}$ of the voltage multiplier and then, from (9), the minimum achievable output power $P_{\rm OUT\,min}$ for correct power matching. In order to be able to achieve power matching with very low output power, we need to use diodes with a small parasitic capacitance, for a fixed minimum diode area in order to reduce ΔC.

Let k be the ratio between $P_{\rm OUT\,min}$ and the maximum dc power required at the output of the voltage multiplier. Now, we can suppose that for the application we are interested in, it is sufficient to have an output power that is k times smaller than $P_{\rm OUT\,min}$. We can consider two options, in order to evaluate the best one for the optimization of the operating range.

A first option (case A) could be to dimension the voltage multiplier and the power-matching network for an output power equal to $P_{\rm OUT\,min}$, although a smaller output power would be sufficient; this would lead to a worse power efficiency and then to a reduction of the operating range, but it allows us to have correct power matching. Indeed, in the case of power matching, the input power of the voltage multiplier can be written as

$$P_{\rm IN} = \frac{P_{\rm EIRP}}{4\pi r^2}A_e \tag{20}$$

where A_e is the effective aperture of the transponder's antenna, r is the distance between reader and transponder, and $P_{\rm EIRP}$ indicates the power at which an isotropic emitter would have to be supplied to generate the same radiation power of the reader antenna ($P_{\rm EIRP}$ is limited by national regulations [7]): a reader antenna with a gain G_T may irradiate a maximum power $P_{\rm EIRP}/G_T$.

The input power of the voltage multiplier can also be written as in (8), considering an output power $P_L = P_{\rm OUT\,min}$. Equating (20) and (8), it is possible to plot the maximum operating range achievable as a function of k.

A second option (case B) is to dimension the voltage multiplier considering an output power $P_L = P_{\rm OUT\,min}/k$; in such a condition, as already said, since the power required at the output of the voltage multiplier is smaller than $P_{\rm OUT\,min}$ (and then $R_{\rm eq}$ is larger than $R_{\rm eq\,max}$), power matching could not be achieved. In order to recover power matching, we can put a resistance R^*, in parallel with the input of the voltage multiplier so that the input resistance of the voltage multiplier becomes smaller than $R_{\rm eq\,max}$. In such a case, the input power is given by summing up the input power $P_{\rm IN}$ of the voltage multiplier, given by (8), and the power dissipated by R^*, as follows:

$$P_{\rm IN} + \frac{V_0^2}{2R^*} = \frac{P_{\rm EIRP}}{4\pi r^2}A_e. \tag{21}$$

Substituting (8) into (21), for $P_L = P_{\rm OUT\,min}/k$, it is possible to plot the maximum operating range achievable as function of k.

Referring to the AMS 0.35-μm integrated circuit (IC) technology with a minimum diode area equal to 1 μm^2, and considering an output voltage of 2 V, an operating frequency of 2.45 GHz, and a Q factor of the *LC* matching network of 10, the minimum output power, $P_{\rm OUT\,min}$, which allows us to achieve the power matching, is 12 μW. From Fig. 8(a), where the maximum operating ranges achievable with each option are plotted as a function of k, we can see that option B is to be preferred,

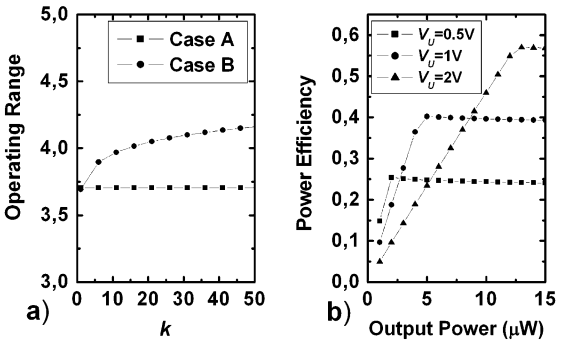

Fig. 8. (a) Maximum operating range as a function of k for the two matching strategies described. (b) Power efficiency of a single-stage voltage multiplier as a function of the output power for three values of the output voltage.

even if some power is dissipated in the resistor R. Fig. 8(a) also tells us that there is no advantage in reducing the power consumption below $P_{\mathrm{OUT\,min}}$, since we cannot reduce the available power required at the antenna. Referring to case B, we plot in Fig. 8(b) the power efficiency of the voltage multiplier as function of the required dc output power. It is possible to note that for small output power, when a resistance is added in parallel with the input of the voltage multiplier, the smaller the output voltage is, the higher is the power efficiency obtained; for larger output power, instead, the larger the output voltage is, the better is the obtained power efficiency.

D. Nonlinear Effects

Because of the nonlinear effects of the voltage multiplier, the current in the antenna I_{ant} also comprises components at frequencies that are integer multiples of the operation frequency. Indeed, the component of the input voltage of the voltage multiplier at the operating frequency f_0 generates an input current I_{in} constituted by the odd harmonic components of f_0. In order to calculate the input current of the voltage multiplier, let us consider a single stage: the input current can be obtained by subtracting the currents in the two diodes across which a voltage V_d, given by (1), drops and by considering the diode model without substrate losses. Then, such current has to be multiplied by the number of stages in order to obtain the total input current I_{in} of the N-stage voltage multiplier, and its expression is given by

$$I_{\mathrm{in}} = NI_S\left[\exp\left(\frac{V_{\mathrm{in}}}{V_T}\right) - \exp\left(-\frac{V_{\mathrm{in}}}{V_T}\right)\right]\exp\left(-\frac{V_U}{2NV_T}\right) + 2N\bar{C}_D\frac{d}{dt}V_{\mathrm{in}}. \quad (22)$$

Exploiting the modified Bessel function series expansion for the two exponential functions that appear in (22), the input current, generated by a sinusoidal input voltage at the operation frequency, can be written as

$$I_{\mathrm{in}} = 4NI_S\exp\left(-\frac{V_U}{2NV_T}\right)\sum_{n=1}^{\infty}B_{2n-1}\left(\frac{V_0}{V_T}\right) \times \cos[(2n-1)\omega_0 t] - 2N\bar{C}_D V_0\omega_0\sin(\omega_0 t). \quad (23)$$

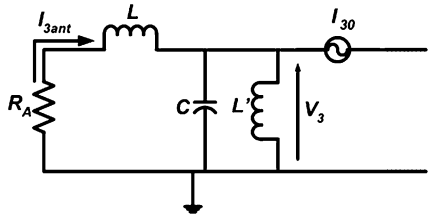

Fig. 9. Equivalent circuit of the system antenna tag to calculate the third harmonic of the antenna's current.

The amplitude of the fundamental of the current in the antenna $I_{1\mathrm{ant}}$ is given by

$$|I_{1\mathrm{ant}}| = I_{10}\sqrt{Q^2+1} \quad (24)$$

where I_{10} is the amplitude of the fundamental of the input current of the voltage multiplier. Let us consider only the effect of the third harmonic $I_{3\mathrm{in}}$ of I_{in}. It is clear that the higher harmonics of the input voltage have the same qualitative behavior, but they are more strongly suppressed by the power-matching network, so that we will take into consideration only $I_{3\mathrm{in}}$. Referring to the equivalent circuit shown in Fig. 9, we can calculate the amplitude of third harmonic of the current in the antenna $I_{3\mathrm{ant}}$ due to $I_{3\mathrm{in}}$. From (23), we can obtain the amplitude of the third harmonic of the current in the antenna $I_{3\mathrm{ant}}$ as

$$|I_{3\mathrm{ant}}| = \frac{3\omega_0 L'(Q^2+1)I_{30}}{\sqrt{(R_{\mathrm{eq}}-9\omega_0 L'Q)^2+9(QR_{\mathrm{eq}}+(1-8Q^2)\omega_0 L')^2}} \quad (25)$$

where I_{30} is the amplitude of $I_{3\mathrm{in}}$. Using (19) and using for the SPICE parameters FC, m, and V_γ, the default values, which are 0.5, 0.31, and 0.69 V, respectively, we can find that for an output voltage close to 1 V, as typical in passive RFID systems, $\Delta C \cong C_{\mathrm{eq}}$. By substituting C_{eq} with ΔC in (18), since the inductance L' resonates with C_{eq}, we find

$$Q\omega_0 L' \gg R_{\mathrm{eq}}. \quad (26)$$

Using (24) and (26), we can rewrite (25) as follows:

$$|I_{3\mathrm{ant}}| = \frac{\sqrt{Q^2+1}}{\sqrt{64Q^4-7Q^2+1}}|I_{1\mathrm{ant}}|. \quad (27)$$

By assuming that the amplitude of the third harmonic of the current in the antenna is 50 times smaller than the amplitude of the fundamental, we obtain that Q has to be larger than 7. If Q is smaller than 7, in order to verify the previous condition, we can place a parallel L^* C^* network in parallel to the input of the voltage multiplier, which resonates at the operating frequency. This network has no effects with respect to the operating frequency but attenuates the harmonics of the current in the antenna. The value of this equivalent capacitance C_n for the nth harmonic is given by

$$C_n = \frac{n^2 C^*}{n^2-1}. \quad (28)$$

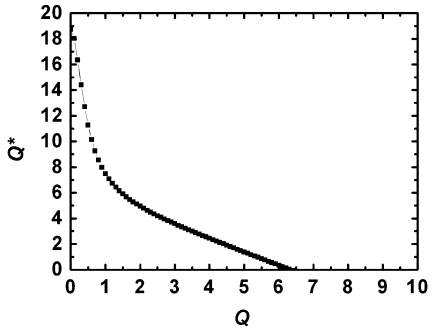

Fig. 10. Quality factor of the parallel resonant L^*C^* network as a function of the quality factor of the power-matching network.

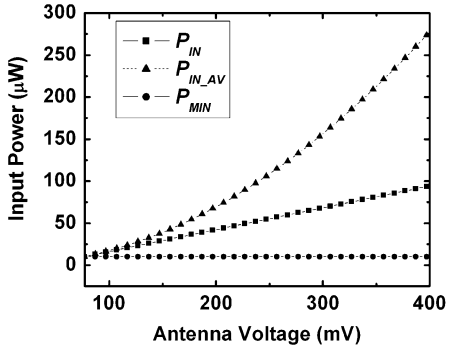

Fig. 11. Required input power versus the amplitude of the antenna voltage for an output voltage of 2 V and an output power of 5 μW.

Using the parallel resonant L^* C^* network, the new expression for the amplitude of the third harmonic of the current in the antenna, as function of the amplitude of the fundamental, using (24), is given by

$$|I_3| = \frac{\sqrt{Q^2+1}}{\sqrt{9\left(Q+\frac{8Q^*}{9}\right)^2+(1-8Q^2-8QQ^*)^2}}|I_1| \quad (29)$$

where $Q^* = \omega_0 R_{\rm eq} C^*$. Assuming that the amplitude of the third harmonic must be at least 50 times smaller than the amplitude of the fundamental, we can derive Q^* as a function of Q. This relationship is shown in Fig. 10. Once Q^* is chosen, the parallel resonant L^* C^* network is dimensioned.

E. Matching When Conditions Vary

The dimensioning of the power-matching network must be done for the maximum operating range when the power available at the terminals of the transponder's antenna is the minimum one that allows the transponder to operate correctly. Then, it is important to analyze what happens when the transponder is moved closer to the reader and the input power of the voltage multiplier increases. As a consequence of such variations, the input equivalent resistance of the voltage multiplier varies, causing mismatch, and so a part of the power available at the antenna's terminals is reflected. It is important to verify that the power that comes to the input of the voltage multiplier is sufficient to ensure its correct operation.

In order to keep the dc supply voltage constant, a series voltage regulator is placed at the output of the rectifier. We can assume that the current in the voltage regulator is much smaller than the current provided at its output and that the minimum voltage drop required across the regulator is only a few tens of millivolts, as can be shown in practical implementations [6]. Therefore, we can consider the efficiency of the voltage regulator practically one at the maximum operating range, and for shorter distances, we can assume that the input current of the voltage regulator is constant and equal to the dc current I_U required by the load. In other words, the output of the rectifier sees the voltage regulator as an ideal dc current generator I_U. Once the power-matching network was dimensioned in the condition of maximum operating range, as previously explained, from (5), for the minimum output power required for the correct operation of the transponder, we can obtain the amplitude of the input voltage V_0, and so from (8) we obtain the input power of the rectifier. Then, once the input power of the voltage multiplier is calculated, we can derive the minimum amplitude of the voltage $V_{S\rm MIN}$ at the antenna, which ensures the correct operation of the transponder and its expression is given by

$$V_{S\rm MIN} = \sqrt{8R_A P_{\rm IN}}. \quad (30)$$

As previously mentioned, when increasing the voltage at the antenna with respect to its minimum value, given by (30), the input resistance of the voltage multiplier varies. In order to calculate the input resistance of the voltage multiplier as a function of the voltage at the antenna, from the circuit of Fig. 7, we can calculate the input power of the voltage multiplier as a function of the voltage at the antenna and of the input resistance of the voltage multiplier. Its expression is given by

$$P_{\rm IN} = \frac{R_{\rm eq}(Q^2+1)}{2(R_A(Q^2+1)+R_{\rm eq})^2}V_S^2 \quad (31)$$

where V_S is the amplitude of the voltage at the antenna's terminals. The input power also has the expression shown in (8), and using (5) to substitute the exponential function that appears in (8), we obtain the following equation:

$$\frac{\sqrt{Q^2+1}}{4I_S(R_A(Q^2+1)+R_{\rm eq})\left(1+\frac{I_U}{I_S}\right)}V_S = \frac{B_1\left(\frac{V_0}{V_T}\right)}{B_0\left(\frac{V_0}{V_T}\right)} \quad (32)$$

where V_0 can be derived from (31) using (9). From (32), by numerical iteration, it is possible to obtain the input resistance of the rectifier as a function of V_S and I_U. Once this result is obtained, from (31), we can derive the input power of the rectifier as a function of V_S and then the amplitude of the input voltage V_0 of the voltage multiplier as a function of V_S. Then, from (5), we can derive the output voltage of the rectifier as a function of V_S. Again, assuming that the antenna is a dipole ($R_A = 72\ \Omega$), the output voltage V_U is equal to 2 V, and the maximum output power P_L is 5 μW, we can calculate, in the condition of maximum operating range, the minimum antenna voltage, and its value is 77 mV. We can plot the power $P_{\rm IN}$ at the input of the voltage multiplier and the power $P_{\rm IN\_AV}$ at the terminals of the antenna when increasing the antenna voltage with respect to its minimum value, given by (30). Both quantities are plotted as a function of V_S in Fig. 11. Of course, in the condition of maximum operating range, for which power matching is achieved, $P_{\rm IN} = P_{\rm IN\_AV}$. When the antenna's voltage increases, part of the power available at the terminals of the antenna, given by

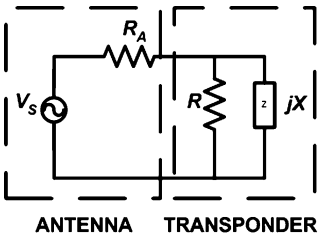

Fig. 12. Equivalent circuit of the antenna and the load represented by transponder.

the difference between the two curves plotted on Fig. 11, is reflected by the power-matching network because of the mismatch due to the variation of the input resistance of the voltage multiplier. Anyway, the input power of the voltage multiplier is always larger than the minimum value $P_{\rm MIN}$ necessary to ensure the correct operation of the transponder.

III. Backscatter Modulator

A. ASK and PSK Backscatter Modulation

In this section, we briefly review ASK and PSK backscatter modulation in order to identify the most appropriate choice for the task at hand. Indeed, referring to Fig. 12 and assuming a minimum scattering antenna, the amplitude of the backscattered power $P_{\rm BS}$ has the expression

$$P_{\rm BS} = \frac{P_{\rm EIRP}}{4\pi r^2} A_e \frac{4R_A^2}{|R_A + jX \,\|\, R|^2}. \tag{33}$$

The impedance seen by the antenna can be represented as a resistance R in parallel with a reactance X, as shown in Fig. 12. If the antenna cannot be considered as a minimum scattering antenna, in order to calculate the backscattered power, in the second term of (33) we have to add another term, which is the backscattered power when the antenna is left open and is independent of the antenna load, so that such term has no effect on the probability of error at the reader.

In the case of ASK modulation, we can assume that the impedance seen by the antenna is real ($X \gg R$) and is modulated by the data signal between two values R_1 and R_2. In order to have equal mismatch in both states, it is sufficient to choose $R_2 = R_A^2/R_1$; in such a condition, in both states, the same power is transferred from the antenna to the load. Assuming $R_2 > R_1$, in order to modulate the resistance seen by the antenna, we can use a switch, driven by the data signal, to connect a resistance $R_{\rm MOD}$ in parallel with the input resistance R_2 of the transponder in such a way that $R_1 = R_2 \| R_{\rm MOD}$. When $R_{\rm MOD}$ is not connected, the antenna sees a resistance R_2 and all the power $P_{\rm IN2}$ transferred from the antenna to the load can be used to supply the transponder; when the resistance $R_{\rm MOD}$ is connected, the antenna sees a resistance R_1, and only a fraction $P_{\rm IN1}$ of the power transferred from the antenna to the load can be used to supply the transponder, while the remaining part is dissipated on the resistance $R_{\rm MOD}$. As a consequence, the power transferred from the antenna to the load remains constant in both states, but $P_{\rm IN1}$ and $P_{\rm IN2}$ are different and are given by

$$\begin{aligned} P_{\rm IN2} &= P_{\rm AV} \frac{4R_A R_2}{(R_A + R_2)^2} \\ P_{\rm IN1} &= P_{\rm AV} \frac{4R_A R_1}{(R_A + R_1)^2} \frac{R_{\rm MOD}}{R_{\rm MOD} + R_2} \end{aligned} \tag{34}$$

where $P_{\rm AV} \equiv P_{\rm EIRP} A_e/(4\pi r^2)$. It is possible to demonstrate that, except for the solution $R_1 = R_2$ (i.e., $R_{\rm MOD} \to \infty$), which would imply the absence of modulation, the equation $P_{\rm IN2} = P_{\rm IN1}$ has no solution. This means that, when modulating, the tag cannot be supplied with constant power. Using the condition $R_2 = R_A^2/R_1$, the backscattered powers $P_{\rm BS1}$ and $P_{\rm BS2}$, when the impedance seen by the antenna are R_1 and R_2, respectively, read

$$P_{\rm BS2} = P_{\rm AV} \frac{4R_A^2}{(R_A + R_2)^2}, \quad P_{\rm BS1} = \frac{R_2^2}{R_A^2} P_{\rm BS2}. \tag{35}$$

We shall see later that the probability of error at the receiver depends on a unique quantity, an effective (or "modulated") power P_U, which is the power of the signal obtained from the demodulation of the voltage directly applied to the radiation resistance of the antenna, again dissipated—for convenience—on a resistance R_A. The larger the value of P_U, the smaller the probability of error. In order to compare the performances of the ASK and PSK backscatter modulation, we can calculate P_U for the ASK modulation, assuming to use a coherent receiver, perfectly equal to the one that will be used for PSK modulation (to be discussed later) except for the detector threshold. Without loss of generality, we can refer to unipolar return-to-zero (RZ) coding for both ASK and PSK modulation: if we transmit an alternating sequence of symbols "0" and "1", the demodulated signal is a square wave whose amplitude varies between $(V_1 - V_2)/2$ and zero. We therefore obtain $P_U = (V_1 - V_2)^2/8R_A$. As a consequence, if the reader's antenna is perfectly matched, P_U has the expression

$$\begin{aligned} P_U &= (\sqrt{8R_A P_{\rm BS1}} - \sqrt{8R_A P_{\rm BS2}})^2/(8R_A) \\ &= P_{\rm BS2} \left(1 - \frac{R_2}{R_A}\right)^2. \end{aligned} \tag{36}$$

In the case of PSK modulation, we must have $R = R_A$ so that the transponder is close to the matching condition, while X is modulated with the data signal. In fact, referring to Fig. 12, the phase θ of the backscattered signal, proportional to the voltage $V_{\rm BS}$ on the radiation resistance R_A, reads

$$\theta = \angle V_{\rm BS} = -a\tan\left\{\frac{R_A X}{R_A^2 + 2X^2}\right\}. \tag{37}$$

If X is modulated symmetrically with respect to zero, so is θ, which implies that the power $P_{\rm BS}$ reflected by the antenna and the power $P_{\rm IN}$ transferred to the transponder remain constant during modulation and are given by

$$P_{\rm BS} = P_{\rm AV} \frac{4\left(R_A^2 + X^2\right)}{R_A^2 + 4X^2} \tag{38}$$

$$P_{\rm IN} = P_{\rm AV} \frac{4X^2}{R_A^2 + 4X^2}. \tag{39}$$

At the receiver, in order to demodulate the PSK signal, we have to use a coherent receiver. As it will be clearer in Section IV, if an alternating sequence of symbols "0" and "1" is transmitted, the demodulated signal is a square wave whose amplitude varies between two states, which are zero and $A\sin(\theta)$, where A is the amplitude of the signal received at the reader,

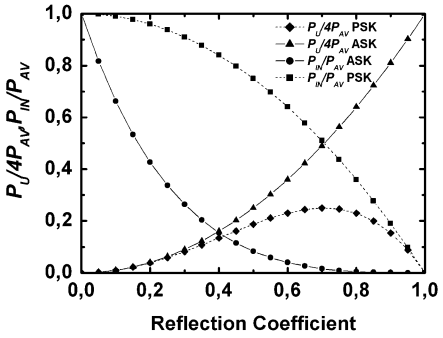

Fig. 13. Effective power P_U at the reader and power $P_{\rm IN}$ transferred to the transponder for the ASK and PSK modulations, as a function of the reflection coefficient.

determined by the backscattered power, and θ is the modulation depth, given by (37). Following the reasoning used for the ASK modulation, the power P_U is given by

$$P_U = 4P_{\rm BS}\sin^2(\theta). \tag{40}$$

In order to compare the performance of ASK and PSK modulation [2], we can plot in Fig. 13, $P_U/4P_{\rm AV}$ for both modulations, as a function of the reflection coefficient ρ, defined as $\rho \equiv |(Z_{\rm IN} - R_A)/(Z_{\rm IN} + R_A)|$, where $Z_{\rm IN}$ is the input impedance of the transponder $Z_{\rm IN} = R \,||\, jX$. Fig. 13 also shows $P_{\rm IN}/P_{\rm AV}$, considering in the case of the ASK modulation the average of $P_{\rm IN1}$ and $P_{\rm IN2}$, assuming that the two states have the same likelihood. It is possible to note that for a given ρ, the PSK backscatter modulation ensures a larger $P_{\rm IN}$, but the ASK backscatter modulation ensures a larger P_U. Since, as we will see later, the most critical aspect limiting the operating range is represented by the input power of the transponder, the PSK backscatter modulation is to be preferred.

Furthermore, PSK backscatter modulation allows us to provide a constant power supply to the transponder during modulation.

Let us note for both ASK and PSK modulations, a coherent receiver would be required at the reader to filter away the unmodulated carrier backscattered by unwanted obstacles (clutter), which is orders of magnitude larger than the backscattered modulated signal to which it adds at the receiver. In such a way, the clutter can be separated by simply multiplying the received signal by the locally synthesized carrier. The alternative option to filter away the clutter would be represented by the use of subcarrier backscatter modulation, which would allow the use of a simpler incoherent receiver, at least for the ASK modulation. However, such solution would have the serious drawback of implying a very large increase of the modulator switching frequency, and therefore of the transponder power consumption, leading to a significant reduction of the operating range.

From now on, we will take in consideration the PSK backscatter modulation.

B. PSK Backscatter Modulator

Most of PSK backscatter modulators [2], [8], [9], independently of their implementation, allow modulation of their output capacitance with the input signal. Referring to Fig. 1, L is used to make the imaginary part of the admittance seen at the output of the modulator symmetric with respect to zero. Therefore, L has to be chosen to resonate with the mean value of the capacitance seen from the output of the modulator when the input signal varying and is therefore

$$L = \frac{1}{(2\pi f_0)^2\left(\frac{C_{V1}+C_{V2}}{2}\right)} \tag{41}$$

where f_0 is the operating frequency and C_{V1}, C_{V2} are the output capacitances of the modulator when the input signal is high and low, respectively. The reactance X is therefore given by

$$X = \frac{2}{(2\pi f_0)|C_{V1} - C_{V2}|}. \tag{42}$$

IV. Modulation Depth and Maximum Operating Range

In this section, we will describe the criteria for choosing the modulation depth in order to maximize the operating range of the tag-reader system. When modulating the impedance seen by the transponder's antenna, it is necessary to ensure that the power at the input of the voltage multiplier is larger than the minimum required for its correct operation, and the probability of error at the receiver is smaller than a given value, required for the correct receiving. A tradeoff has to be found between the two conditions in order to maximize the operating range.

A. Transponder Input Power

Referring to Fig. 12, the power $P_{\rm IN}$ transferred from the antenna to the input of the transponder is given by (39). In order to ensure the correct operation of the transponder, $P_{\rm IN}$ must be larger than the minimum power required for the transponder operation, consisting of the sum of the power $P_{\rm MOD}$ dissipated by the modulator and the power $P_{\rm DIG}$ dissipated by the digital section, divided by the efficiency η previously calculated. As consequence, the following relation has to be fulfilled:

$$\frac{P_{\rm EIRP}}{4\pi r^2}A_e\frac{4X^2}{R_A^2 + 4X^2} > \frac{1}{\eta}(P_{\rm MOD} + P_{\rm DIG}). \tag{43}$$

From (43), it is evident that the larger the power efficiency of the transponder, the larger the range of values of X that satisfy (43). Equation (43) gives a first condition that has to be fulfilled by X in order to ensure the correct operation of the tag-reader system. The other condition will be given by the probability of error at the receiver.

B. Probability of Error at the Reader

1) Received Signal at the Reader's Antenna: As already said, the signal received by the reader's antenna has two components: a PSK backscattered signal and an unmodulated carrier. The PSK backscattered signal $x_{\rm BS}(t)$ coming from the transponder's antenna has a carrier frequency equal to the operating frequency of the RFID system and a phase, which belongs to a group of two values symmetric with respect to zero and with an absolute value θ given by (37). The amplitude of such a signal can be calculated from the amplitude of the power backscattered by the transponder's antenna, taking into

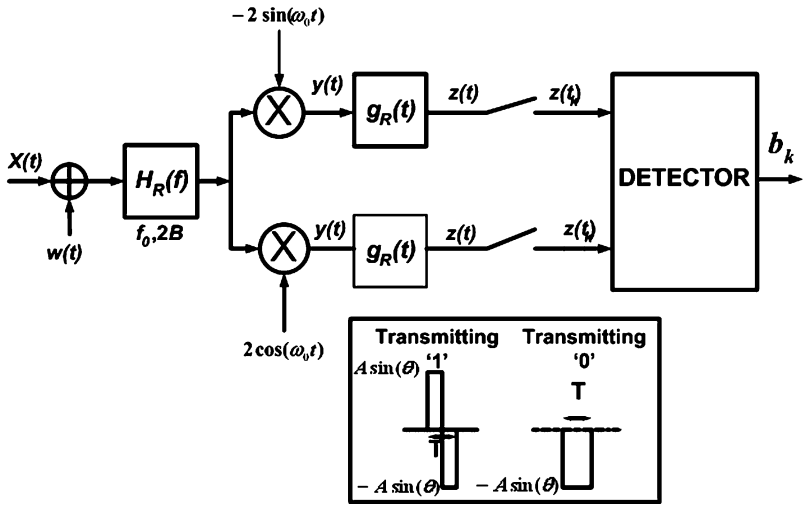

Fig. 14. PSK receiver architecture (insert: elementary impulse when transmitting "0" and "1").

consideration the free-space attenuation. Assuming that the reader's antenna is perfectly matched with the reader, the amplitude A of the signal $x_{\rm BS}(t)$ is given by the expression

$$A = \frac{A_e}{2\pi r^2}\sqrt{\frac{2R_A\left(R_A^2+X^2\right)}{R_A^2+4X^2}P_{\rm EIRP}}. \tag{44}$$

Therefore, $x_{\rm BS}(t)$ reads

$$x_{\rm BS}(t) = \sum_{i=0}^{\infty} A\,\text{rect}\left(\frac{t-T/4-iT/2}{T/2}\right)\cos(2\pi f_0 t+\alpha_i) \tag{45}$$

where $\alpha_i \in \{-\theta,\theta\}, 1/T$ is the data rate and $\text{rect}(t/T)$ is a square impulse with an amplitude equal to 1, a duration T, and it is centered at $t=0$. The unmodulated carrier $x_{\rm UM}(t)$ that comes back to the reader's antenna is a sinusoidal voltage with an amplitude B and a phase β completely unknown, as follows:

$$x_{\rm UM}(t) = B\cos(2\pi f_0 t+\beta). \tag{46}$$

The complete received signal $x(t)$ at the reader's antenna is obtained by summing up the two components. Since the unmodulated carrier $x_{\rm UM}(t)$ has a power level much larger than the PSK backscattered signal, in order to generate the local carrier required to downconvert the received signal, it is not possible to use a phase-locked loop (PLL) because it would reproduce the unmodulated carrier. A possible solution is to transmit, at the beginning of each data package, a preamble, which is, for example, a sequence of symbols "1" known to the reader and to use an adaptive system that varies the phase of the locally generated carrier until the signal at the output of the filter has the correct amplitude. In this situation, the local oscillator is synchronized with the received PSK signal and generates a sinusoidal voltage at the operating frequency with a phase equal to the mean value of the phase of the received PSK signal. Assuming the use of unipolar RZ coding, as will be described later, if we transmit, as already said, a sequence of symbols "1", the carrier generated locally has a zero phase; using an oscillator with quadrature outputs, it is possible to generate the oscillations for the two branches of the receiver. The receiver has to be able to remove the unmodulated signal, which would introduce an error in the demodulation due to its random phase.

2) Receiver Architecture: The scheme of the PSK receiver is shown in Fig. 14 [4]. We consider an additive white Gaussian noise (AWGN) input noise $w(t)$. Since the phase of the backscattered signal $x_{\rm BS}(t)$ belongs to a group with two values symmetrical with respect to zero, the lower branch of the receiver has no effect since the co-sinusoidal function is an even function and cannot detect the phase variation. By multiplying the input signal $x(t)$ by the locally generated carrier, in quadrature with the received signal and considering only the low-frequency component, which will be the only one to survive after filtering, we obtain that the signal $y(t)$ at the input of the filter $g_R(t)$ is given by

$$y(t) = \sum_{i=0}^{\infty} A\,\text{rect}\left(\frac{t-T/4-iT/2}{T/2}\right)\sin(\alpha_i)+B\sin(\beta). \tag{47}$$

The receiver must be able to remove the unmodulated signal, which would introduce an error in the demodulation due to the random phase. To this aim, the baseband receiver filter must have a zero-average impulse response to block the unmodulated carrier. Since the impulse response of the filter has to be equal to the elementary impulse of one of the two symbols, the previous condition imposes an appropriate choice of the data coding, in which at least a symbol has zero mean value. The most common codes, such as Manchester, unipolar RZ coding, differential bi-phase (DBP), and Miller coding, verify such a condition [1]. Now, in order to obtain numerical results, we can choose one of the previous coding schemes and calculate the probability of error after choosing a proper receiving filter. As an example, without loss of generality, we consider a unipolar RZ coding: in such a case, the elementary impulse $p_1(t)$, when transmitting a bit "1", is obtained by transmitting a symbol θ and a symbol $-\theta$, in sequence. Instead, the elementary impulse $p_0(t)$, when transmitting a bit "0", is obtained by transmitting two symbols $-\theta$ in sequence. The two elementary impulses are

shown in the insert of Fig. 14. Now, we choose the impulse response of the filter $g_R(t)$ with the same waveform of the elementary impulse associated to the transmission of "1". Since the filter $g_R(t)$ amplifies or attenuates the signal and the noise in the same manner, we can suppose that the amplitude of the impulse response of the filter is equal to $1/T$. In this condition, the frequency response $G_R(f)$ of the filter is given by,

$$G_R(f) = \frac{1}{2}\sin c\left(\frac{fT}{2}\right)\exp\left(-j\omega\frac{T}{4}\right) \times\left[\exp\left(-j\omega\frac{T}{2}\right)-1\right] \quad (48)$$

where $\sin c(x) = \sin(\pi x)/(\pi x)$. Once the impulse response of the filter is fixed, we can derive the expression of the signal $z(t)$ at the output of the filter, when transmitting "1" and "0". The expressions of the signals $z_1(t)$ and $z_0(t)$ at the output of the filter when transmitting "1" and "0", respectively, are given by

$$z_1(t) = p_1(t)\otimes g_R(t), z_0(t) = p_0(t)\otimes g_R(t). \quad (49)$$

By sampling the signal, at the output of the filter at time instants $t_k = kT$ (k is an integer), the signal at the input of the detector is zero when transmitting "0" and $A\sin(\theta)$ when transmitting "1". Since the unmodulated carrier provides a constant component at the input of the filter, exactly as it occurs when transmitting "0", after the convolution and the sampling it gives a zero signal. Supposing that the transmissions of "0" and "1" have the same likelihood, the detector's threshold can be chosen in the middle between $z_1(t_k)$ and $z_0(t_k)$, according to the MAP criterion [4]. Supposing that the noise has a zero mean value and a standard deviation σ, the probability of error P_{e0} when transmitting "0" and the probability of error P_{e1} when transmitting "1" are given by

$$P_{e0} = P_{e1} = \mathrm{erf}\left(\frac{A/2\sin(\theta)}{\sigma}\right) = \mathrm{erf}\left(\frac{\sqrt{R_A P_U}}{\sqrt{2}\sigma}\right) \quad (50)$$

where $\mathrm{erf}(x)$ is the error function. Since the two symbols "0" and "1" have the same likelihood, the total probability of error is equal to each probability of error when transmitting "0" and "1".

Following the same procedure in the case of a Manchester coding scheme and choosing the receiving filter in the same manner, one obtains, after the sampling, for the two symbols the two levels $\pm A\sin(\theta)$ and then a smaller probability of error.

In the case of ASK backscatter modulation, using the receiver shown in Fig. 14 and the unipolar RZ coding, we would obtain the following expression for the total error probability P_e:

$$P_e = \mathrm{erf}\left(\frac{V_1 - V_2}{4\sigma}\right) = \mathrm{erf}\left(\frac{\sqrt{R_A P_U}}{\sqrt{2}\sigma}\right). \quad (51)$$

As already said and as evident from (50) and (51), the parameter P_U calculated in Section III is the only parameter of the backscatter modulator affecting P_e.

3) Noise Spectral Density: We can suppose that the noise at the input of the receiver is due to the thermal noise of the antenna, followed by an amplifier with a noise figure F and with a gain sufficiently high to allow us to neglect the noise figure of the following stages. In such a condition, the expression of the noise spectral density $N_{0\mathrm{th}}$ is given by

$$N_{0\mathrm{th}} = 2Fk_BTR_A \quad (52)$$

where k_B is the Boltzmann constant and T is the absolute temperature. If the input noise is a white Gaussian noise with a power spectral density equal to $N_{0\mathrm{th}}$, its power spectral density after filtering is obtained by multiplying the power spectral density at the input by the square absolute value of the frequency response $G_R(f)$ of the filter. As a consequence, the standard deviation σ of the noise at the output of the filter is obtained by integrating the power spectral density as follows:

$$\sigma^2 = N_{0\mathrm{th}}\int_{-\infty}^{+\infty}|G_R(f)|^2 df. \quad (53)$$

We can now consider the phase noise due to the local oscillator. The carrier generated by the frequency synthesizer is not perfectly monochromatic, due to the phase noise. The power spectrum density of the phase noise goes down, initially, as $1/f^3$ due to the flicker noise of the devices in the oscillator, then as $1/f^2$ due to the thermal noise of the devices in the oscillator, with a typical corner frequency of some hundreds of kilohertz [10].

Since the reader uses the same oscillator to generate the transmitted carrier and the local oscillation, the phase noise that affects the received signal and the local oscillation, used to downconvert the received signal, are generated by the same oscillator but in different time instants with a certain delay ΔT. As a consequence, after the downconversion, the low-frequency component is given by

$$V(t) = V_{\mathrm{IN}}(t)V_{\mathrm{OL}}(t)|_{\mathrm{low}} = A\sin[\theta+\varphi(t)-\varphi(t-\Delta T)]. \quad (54)$$

Now, we have to study the variance of $\varphi(t)-\varphi(t-\Delta T)$. Its power spectral density $S(f)$ is given by

$$S(f) = S_\varphi(f)|1-\exp(-j\omega\Delta T)|^2 = 4S_\varphi(f)\sin^2\left(\frac{\omega}{2}\Delta T\right). \quad (55)$$

In general, we can write the power spectral density $S_\varphi(f)$ of the phase noise $\varphi(t)$ as a sum of a $1/f^3$ component and a $1/f^2$ component, imposing that the two components are equal at the corner frequency f_c. The expression of $S_\varphi(f)$ is

$$S_\varphi(f) = \frac{A}{f^2} + \frac{Af_c}{f^3}. \quad (56)$$

By substituting the two components of $S_\varphi(f)$ in (55) and integrating in frequency, we can calculate the variance σ_w^2 associated to the $1/f^2$ component of the power spectral density of the phase noise and the variance $\sigma_{1/f}^2$ associated to the $1/f^3$ component of the power spectral density of the phase noise. In the case of open-loop voltage-controlled oscillator (VCO), from [11] we can derive σ_w^2, whose expression is given by

$$\sigma_w^2 = 4\pi^2 A\Delta T[\mathrm{rad}^2]. \quad (57)$$

As one can expect, the power of the jitter associated to the $1/f^2$ component is proportional to the delay. In the case of open-loop VCO, an approximate expression of the power of the jitter associated to the $1/f^3$ component is given in [12], and its expression is

$$\sigma^2_{1/f} = 4\pi^2\alpha^2 A f_c \Delta T^2 [\mathrm{rad}^2] \tag{58}$$

where α is a dimensionless parameter typically close to 5 [12]. Now, we can calculate the variance of $\varphi(t) - \varphi(t - \Delta T)$ by summing up the $1/f^2$ and the $1/f^3$ components of the power spectral density of the phase noise. We can then define φ as the maximum value of $\varphi(t) - \varphi(t - \Delta T)$, given by $\varphi = \sqrt{2(\sigma_w^2 + \sigma_{1/f}^2)}$. In the case of RFID systems, since the operating range is a few meters (especially for the systems operating at 2.45 GHz), the delay is small with respect to $1/f_C$ and then the variance of the jitter is mainly due to the $1/f^2$ component. Such a result was obtained by considering an open-loop VCO. In the case of a closed-loop PLL, the power spectral density of the phase noise is filtered by the transfer function of the PLL, and the variance is even smaller, so that the open loop VCO represents the worst case.

The phase jitter causes a shift of the constellation of symbols, leading to an error in the detection. Indeed, in the presence of a phase jitter φ, the level associated to the transmission of a symbol "0" remains zero and the level associated to the transmission of a symbol "1" becomes $[A\sin(\theta)\cos(\varphi)]$ rather than $A\sin(\theta)$. According to the MAP criterion, since the two symbols have the same likelihood, the threshold of the detector is chosen in the middle of the two levels in absence of phase noise, and then the probability of error when transmitting "0" is given by (50), while the probability of error when transmitting "1" is given by

$$P_{e1} = \mathrm{erf}\left(\frac{A\sin(\theta)(2\cos(\varphi) - 1)}{2\sigma}\right). \tag{59}$$

The total probability of error is given by the mean value of the probabilities of error when transmitting "0" and "1". In order to ensure reasonable receiver performance, the total probability of error has to be smaller than a given probability of error P_e*, as follows:

$$P_e = \frac{1}{2}\left\{\mathrm{erf}\left(\frac{A\sin(\theta)(2\cos(\varphi) - 1)}{2\sigma}\right)\mathrm{erf}\left(\frac{A\sin(\theta)}{2\sigma}\right)\right\} < P_e*. \tag{60}$$

Since A and θ are functions of X, (60) gives us another condition to find the values of X that ensures acceptable operation of the transponder–reader system.

Considering that the RFID system has an operating frequency of 2.45 GHz or 868 MHz, the maximum allowed P_{EIRP} for the reader is 500 mW according to European regulations [7]. We also assume that the transponder antenna is a $\lambda/2$ dipole, which has a radiation resistance of 72 Ω and an effective aperture of $0.13\lambda^2$ [1]. Furthermore, using a single-stage voltage multiplier, the power efficiency is about 15% [13]. Then, we assume that

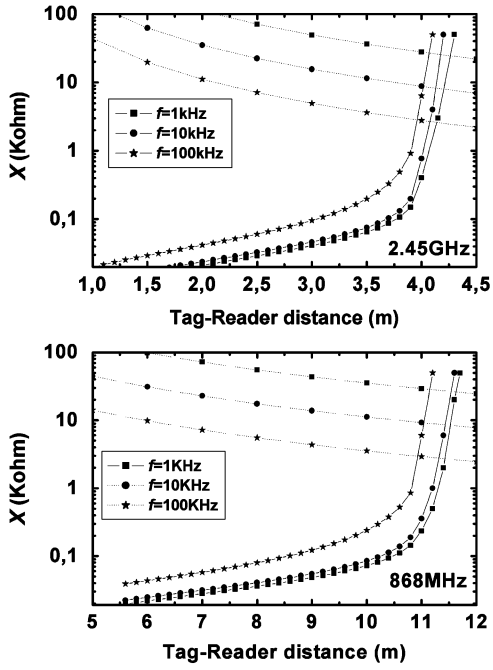

Fig. 15. X values that satisfy the (43) and (60) as a function of the distance between reader and transponder for three different data rates for an operating frequency of 868 MHz (top) and 2.45 GHz (bottom).

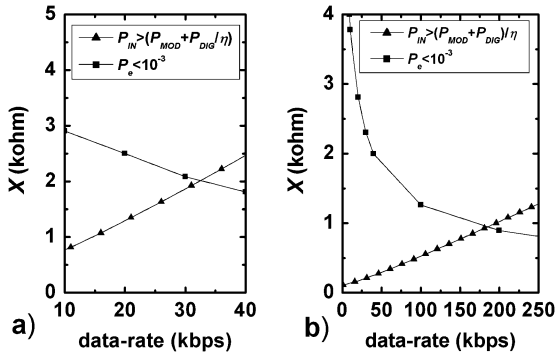

Fig. 16. X values that satisfy the (43) and (60) as a function of the frequency of the data signal (a) for an operative range of 4 m and an operating frequency of 2.45 GHz and (b) for an operative range of 11 m and an operating frequency of 868 MHz.

the supply voltage is 0.6 V, and the power P_{DIG} is equal to 1 μW. We also assume that $T = 300$ K, $R_A = 72\ \Omega$, and $F = 5$ dB, $N_{0\mathrm{th}}$ is equal to 1.88 nV^2/Hz, and $P_e* = 10^{-3}$. In such conditions, we can plot the values of X that satisfy (43) and (60), as function of the distance r between reader and transponder. The diagram is shown in Fig. 15 for different data rates: pairs of X and r that satisfy (43) and (60) lie between the two curves for a fixed data rate. In particular, the values of X that satisfy (43) have, as lower boundary, the continuous curve corresponding to the considered data rate; on the other hand, the values of X that satisfy (60) have, as upper boundary, the dashed curve corresponding the considered data rate. From Fig. 15, it is clear that by reducing the data rate, the range for a fixed X becomes larger because the power required by the transponder, for the modulation and the digital section, decreases and because the bandwidth of the receiving filter becomes smaller, leading to

a smaller noise power at its output and then to a smaller error probability.

From Fig. 15, it is possible to note that by a proper choice of the modulation depth, the operating range, for a passive RFID system, which works in the microwave range, is larger than 4 m, while for a passive RFID system, which works in the UHF frequency range, is larger than 11 m. It is also possible to find the maximum data rate, once the operating range is fixed. For example, we can choose an operating range of 4 m, and we can plot the two curves that satisfy (43) and (60) as function of the data rate in order to obtain the value of X that allow us to maximize the data rate for the chosen operating range. Such a diagram is shown in Fig. 16, for an operating frequency of 2.45 GHz and 868 MHz: the region with acceptable values of X is the one comprised between the two curves. It is possible to note that, for an operating range of 4 m and for an operating frequency of 2.45 GHz, the maximum data rate is about 30 Kb/s; while, for an operative range of 11 m and for an operating frequency of 868 MHz, the maximum frequency of the data signal is about 180 kb/s. If U.S. regulations are considered, which provide a maximum allowed P_{ERP} of 4 W, the same considerations lead to a maximum operating range of about 11 m at 2.45 GHz and 29 m at 916 MHz, for a data rate of a few tens of kilobits per second.

V. Conclusion

This paper has presented an analysis and a discussion of the design options and tradeoffs for a passive microwave transponder. A set of criteria was derived for the optimization of the voltage multiplier, the power-matching network, and the backscatter modulator in order to optimize the operating range, once the data rate is fixed or, to optimize the data rate, once the operative range is chosen. We have also shown that radio frequency identification (RFID) transponders, which require a dc power of 1 μW for the digital section, may reach an operating range of about 4 m in the ISM 2.45-GHz band and 11 m in the ISM 868-MHz band, for a data rate of several kilobits per second and, according to European Union regulations. Present U.S. regulations would allow us to obtain an almost tripled operating range. Such performances in terms of operating range, data rates, and cost might open promising perspectives for the deployment of passive RFID systems even in ambient intelligence or ubiquitous computing scenarios and in outdoor applications.

Acknowledgment

The authors would like to thank with Dr. P. Andreani, DTU Lyngby, Denmark, for fruitful discussions.

References

[1] K. Finkenzeller, *RFID Handbook: Fundamentals and Applications in Contactless Smart Cards and Identification*, 2nd ed. New York: Wiley, 1999, pp. 117–126, 143–148, 183–186.

[2] U. Karthaus and M. Fischer, "Fully integrated passive UHF RFID transponder IC with 16.7-μm minimum RF input power," *IEEE J. Solid-State Circuits*, vol. 38, no. 10, pp. 1602–1608, Oct. 2003.

[3] M. Abramowitz and I. A. Stegun, *Handbook of Mathematical Functions with Formulas, Graphs and Mathematical Tables*, 9th ed. New York: Dover, 1972, pp. 358–364.

[4] B. Razavi, *RF Microelectronics*. Upper Saddle River, NJ: Prentice Hall PTR, 1997, pp. 74–93.

[5] SPICE MOS Model BSIM3v3 [Online]. Available: http://www.device.eecs.berkeley.edu/~bsim3

[6] G. De Vita and G. Iannaccone, "Ultra-low-power RF section of a passive microwave RFID transponder in 0.35 μm BiCMOS," presented at the IEEE Int. Symp. Circuits Systems (ISCAS 2005), Kobe, Japan, May 2005.

[7] *Electromagnetic Compatibility and Radio Spectrum Matters (ERM); Short Range Devices (SRD); Radio Equipment to Be Used in the 25 MHz to 1000 MHz Frequency Range With Power Levels Ranging Up to 500 mW*. ETSI EN 330 220-1.

[8] M. Kossel, "Microwave backscatter modulation systems," in *2000 IEEE MTT-S Int. Microwave Symp. Dig.*, Boston, MA, Jun. 2000, pp. 11–16.

[9] M. Kossel, "An active tagging system using circular polarization modulation," *IEEE Trans. Microw. Theory Tech.*, vol. 47, no. 12, pp. 2242–2248, Dec. 1999.

[10] F. Svelto and R. Castello, "A bond-wire inductor-MOS varactor VCO tunable from 1.8 to 2.4 GHz," *IEEE Trans. Microw. Theory Tech.*, vol. 50, no. 1, pp. 403–407, Jan. 2002.

[11] U. K. Moon, K. Mayaram, and J. T. Stonick, "Spectral analysis of time-domain phase jitter measurements," *IEEE Trans. Circuits Syst.*, vol. 49, no. 5, pp. 321–327, May 2002.

[12] C. Liu and J. A. McNeill, "Jitter in oscillators with $1/f$ noise sources," in *Proc. 2004 Int. Symp. Circuits Systems*, Vancouver, BC, Canada, May 2004, pp. 773–776.

[13] G. De Vita and G. Iannaccone, "Design criteria for the RF section of long range passive RFID systems," in *Proc. IEEE NORCHIP Conf. 2004*, Oslo, Norway, Nov. 2004, pp. 107–110.

Giuseppe De Vita was born on March 7, 1978. He received the "Laurea" degree (*cum laude*) in electrical engineering from the University of Pisa, Italy, in 2003. He is currently working toward the Ph.D. degree at the University of Pisa.

He is currently working on the design of passive radio frequency identification (RFID) transponders.

Giuseppe Iannaccone (M'98) was born on April 28, 1968. He received the "Laurea" degree (*cum laude*) in electrical engineering and the Ph.D. degree from the University of Pisa, Italy, in 1992 and 1996, respectively, with a dissertation on transport and noise phenomena in nanoelectronic devices.

Since January 2001, he has been an Associate Professor at the Information Engineering (Electrical Engineering) Department, University of Pisa. His interests include transport and noise modeling in nanoscale devices, devices and architectures for nanoelectronics, the design of passive radio frequency identification (RFID) transponders, and the exploitation of quantum effects in conventional electron devices. He has authored more than 90 papers in peer-reviewed journals and more than 50 papers in proceedings of international conferences.

Dr. Iannaccone has participated in a series of European and national research projects as consortium coordinator or principal investigator.